


Beliaev Damping of a Spin-Orbit-Coupled Bose-Einstein Condensate

Rukuan Wu and Zhaoxin Liang*

Department of Physics, Zhejiang Normal University, Jinhua, 321004, China

 (Received 4 March 2018; revised manuscript received 22 July 2018; published 30 October 2018)

Beliaev damping provides a fundamental mechanism for dissipation of quasiparticles. Previous research has shown that the two-component internal degrees of freedom has no nontrivial effect on Beliaev damping. Here we provide the first example where the spinor nature of Bose gases can manifest itself in the Beliaev damping by way of spin-orbit coupling. We identify novel features of the Beliaev decay rate due to spin-orbit coupling; in particular, it shows an explicit dependence on the spin-density interaction and diverges at the interaction-modified phase boundary between the zero-momentum and plane wave phases. This represents a manifestation of the effect of spin-orbit coupling in the beyond-mean-field regime, which by breaking Galilean invariance couples excitations in the density and spin channels. We further show that the measurement of the Beliaev damping rate is experimentally feasible through the measurement of spin polarizability susceptibility, which has been already achieved in spin-orbit-coupled Bose gases.

DOI: [10.1103/PhysRevLett.121.180401](https://doi.org/10.1103/PhysRevLett.121.180401)

The dissipation of quasiparticles through their mutual interactions lies at the foundational aspect of quantum many-body physics [1]. A paradigmatic example is Beliaev damping [2,3] in a superfluid [4], where a quasiparticle disintegrates into two quasiparticles at zero temperature. The investigation of the Beliaev damping rate can offer crucial insights into the basic properties of different many-body systems, e.g., transport and thermalization, as has been demonstrated in a wide variety of systems, ranging from the Bose [5–8] and Fermi superfluids [9–11] and the mixture of Bose-Einstein condensates (BECs) with normal Fermi gas [12–15] to dipolar BECs [16–18] and nonequilibrium polariton BECs [19]. However, previous research on spinor Bose gases have concluded that the two-component internal degrees of freedom (d.o.f.) [20,21], a key ingredient playing out in modern physics, seems to play no role in affecting Beliaev damping, as the damping rates in one- and two-component Bose gases are formally the same. Instead, the aim of this Letter is to show that, by the mechanism of spin-orbit coupling, the two-component internal d.o.f. can manifest itself in Beliaev damping.

The second motivation of this Letter comes from recent experimental realizations of spin-orbit coupling (SOC) with ultracold quantum gases [22–29], which opens new routes toward exotic quantum many-body systems in gauge fields [30–36]. The SOC, where the motion of particles are coupled to their spin, breaks the Galilean invariance [35,37–39], giving rise to a double-minimum single-particle energy spectrum. Thus, a SOC BEC has the crucial novelty already at the mean-field level compared to the SOC-free counterpart [8], which has been intensively studied [22–25,28–32,35,36]. In particular, (i) in the ground state, an exotic stripe phase [29,40–42] spontaneously breaking translational symmetry can emerge, and

(ii) for noninteracting quasiparticles, a softening of phonon or roton modes occurs [43]. More importantly, the critical superfluid velocity cannot be well defined [35,38,39] without *a priori* choice of reference frame. Beyond the mean field, however, the consequence of SOC coupling the spin and motional d.o.f. on the dissipation of quasiparticles, such as Beliaev damping, remains unexplored.

In this Letter, we present the first analytical result on the Beliaev decay of phonons in a SOC BEC [see Eq. (7)]. Moreover, we show that this decay rate is of immediate experimental relevance, as it has a direct connection with the spin polarizability susceptibility, for which measurement has already been achieved [26] in SOC BEC. Specifically, considering the condensate in the zero-momentum phase [23], we find that the damping of phonons, while maintaining the familiar q^5 scaling with momenta, exhibits two novel features in contrast to the SOC-free counterpart. First, the damping rate becomes explicitly dependent on the interaction constant—to be precise, the strength of the spin-density interaction. Remarkably, the damping rate diverges at the critical point that exactly corresponds to the interaction-modified phase boundary between the plane wave and zero-momentum phases. Second, the damping of phonons becomes strongly anisotropic. The former is a result of SOC coupling the density and spin-density excitations due to an absence of Galilean invariance, while the latter is a manifestation of the SOC-induced anisotropic effective mass. While SOC-induced lacking Galilean invariance and anisotropy have been previously investigated in BECs, our present Letter reveals their manifestations beyond the mean-field framework.

Beliaev Damping—For a quasiparticle carrying momentum \mathbf{q} , its decay rate in the Beliaev process at zero temperature can be computed by (see Supplemental Material [44])

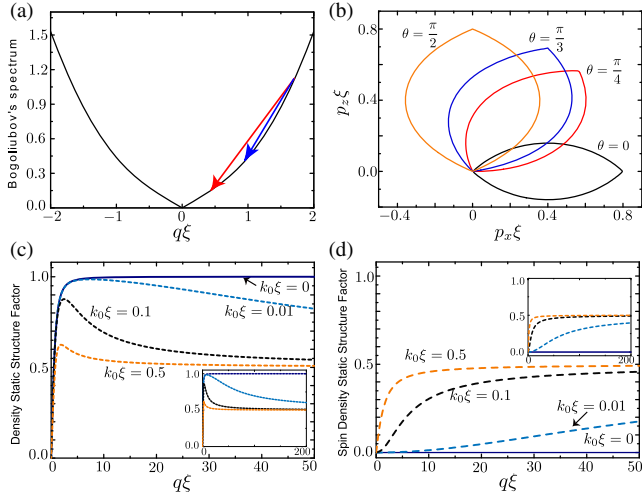


FIG. 1. (a) Dispersion of density mode in the SOC BEC [see Eq. (3)] in the zero-momentum phase. Arrows schematically show the Beliaev decay of a Bogoliubov mode with momentum \mathbf{q} into two modes with momenta \mathbf{p} and $\mathbf{q}-\mathbf{p}$, respectively. (b) The momentum \mathbf{p} manifold allowed by the energy and momentum conservations in the p_x - p_z plane, considering various directions of the initial momentum \mathbf{q} . Specifically, we fix the modulus of \mathbf{q} as $q\xi = 0.8$, while varying its angle θ with respect to the SOC direction along the x axis. For SOC strength, we take $k_0\xi = 0.5$. (c) Density and (d) spin-density static structure factor as a function of q for various k_0 . Here, $\theta = 0$ is taken for illustration. Insets plot the asymptotic behavior of corresponding static structure factors at large momenta. In all plots, the momentum is measured in units of the inverse coherence length ($\xi^{-1} = \sqrt{\hbar/m\Omega}$). For other parameters, we take $G_1/\hbar\Omega = 0.1$ and $G_2/\hbar\Omega = 0.025$.

$$\gamma_B(\mathbf{q}) = \frac{\pi}{2} \sum_{\mathbf{p}, \mathbf{p}'} |B_{\mathbf{p}\mathbf{p}'}|^2 \delta(\epsilon_{\mathbf{q}} - \epsilon_{\mathbf{p}} - \epsilon_{\mathbf{p}'}) \delta_{\mathbf{q}, \mathbf{p}+\mathbf{p}'}. \quad (1)$$

Here, $B_{\mathbf{p}\mathbf{p}'}$ is the matrix element associated with the scattering process wherein a quasiparticle having momentum \mathbf{q} collides with the condensate creating two quasiparticles with momenta \mathbf{p} and \mathbf{p}' [see Fig. 1(a)]. The summation is performed over all possible states allowed by the energy and momentum conservation conditions specified in the δ function and $\delta_{\mathbf{q}, \mathbf{p}+\mathbf{p}'}$, respectively.

To gain insight into how SOC affects Beliaev damping of low-energy excitations of BEC, we recall the classic result of the decay rate in a uniform one-component BEC with condensate density n_0 [45–47], i.e.,

$$\gamma_0 = \frac{3q^5}{640\pi\hbar^3 mn_0}, \quad (2)$$

which exhibits the well-known q^5 scaling. Notice that the formula does not contain the interaction strength between bosonic atoms, rather, the role of interaction comes in only implicitly via n_0 [48]. Equation (2) also holds for a

two-component BEC without SOC in the unpolarized phase [20,21]. There, the density excitation is decoupled from the spin-density excitation; hence both the scattering matrix element and the conservation condition in Eq. (1) bear the same form as the one-component case apart from a renormalized interaction constant, which, according to Eq. (2), does not alter the formal result. We remark that a two-component BEC is different from a three-component BEC in that the latter exhibits a spin-flip process [49,50].

By contrast, as we will elaborate below, adding SOC will bring two fundamental differences: (i) the SOC breaks Galilean invariance, resulting in hybridized excitations in density and spin channels, so that the wave functions of low-energy quasiparticles and thus the Beliaev scattering matrix are strongly modified, and (ii) the SOC renders a spatially anisotropic distribution of scattering states allowed by energy and momentum conservation.

Model Hamiltonian—We consider a 3D spatially uniform BEC with a spin-orbit coupling along the x axis. The relevant grand-canonical Hamiltonian is [32,35]

$$K = \int d^3\mathbf{r} \hat{\psi}^\dagger(\mathbf{r}, t) (H_0 - \mu N) \hat{\psi}(\mathbf{r}, t) + \frac{1}{4} \int d^3\mathbf{r} (g + g_{12}) \hat{n}^2(\mathbf{r}, t) + (g - g_{12}) \hat{S}_z^2(\mathbf{r}, t). \quad (3)$$

Here, $\hat{\psi}^\dagger(\mathbf{r}, t) = (\hat{\psi}_1^\dagger, \hat{\psi}_2^\dagger)^T$ and $\hat{\psi}(\mathbf{r}, t) = (\hat{\psi}_1, \hat{\psi}_2)$ are the creation and annihilation operators for the two-component bosonic atoms; $\hat{n}(\mathbf{r}, t) = |\hat{\psi}_1|^2 + |\hat{\psi}_2|^2$ and $\hat{S}_z(\mathbf{r}, t) = |\hat{\psi}_1|^2 - |\hat{\psi}_2|^2$ denote the total and spin-density operators, respectively. The g and g_{12} denote the intra- and interspecies coupling constant, respectively, with $g \neq g_{12}$ in view of relevant experiments [23]. The single-particle Hamiltonian H_0 contains a Zeeman term and an equal contribution of Rashba and Dresselhaus spin-orbital coupling in the x direction [23,41,42,51–53], i.e.,

$$H_0 = \frac{1}{2m} [(p_x - \hbar k_0 \sigma_z)^2 + p_\perp^2] + \frac{\hbar\Omega}{2} \sigma_x, \quad (4)$$

where m is the bare mass of bosonic atoms, σ_i are standard Pauli matrices, and k_0 labels the strength of the SOC. The Hamiltonian of such form has been recently realized in atomic setup [22–29] employing two counterpropagating Raman lasers, where Ω is the Raman coupling constant and k_0 is the momentum transfer between the lasers. We will moreover denote $G_1 = (g + g_{12})n_0/4$ and $G_2 = (g - g_{12})n_0/4$ with n_0 as the condensate density.

Before continuing, let us briefly describe the ground-state properties of the Hamiltonian (3). For $\hbar\Omega < 2\hbar^2 k_0^2/m$, the single-particle dispersion H_0 exhibits degenerate double minima at momenta $p_x = \pm \hbar k_1$ with $k_1 = k_0 \sqrt{1 - m^2(\hbar\Omega)^2/4\hbar^4 k_0^4}$. In this regime, the ground state can exhibit a stripe phase [29] or a plane wave phase [23]. For $\hbar\Omega > 2\hbar^2 k_0^2/m$, the single-particle dispersion features

a global minimum at $k_1 = 0$ and is anisotropic. In this case, the condensate is in the zero-momentum phase [41], described by the familiar order parameter $\phi_0 = (\phi_1^0, \phi_2^0) = \sqrt{n_0/2}(1, -1)$.

Beliaev damping in presence of SOC—Our goal is to investigate the Beliaev damping of the model system. We will assume $\hbar\Omega > 2\hbar^2 k_0^2/m - 4G_2$ [41] when the BEC is in the zero-momentum ground-state phase, which represents the simplest case capturing the essential effect of SOC on the dissipation of quasiparticles as mentioned earlier.

We will first discuss the energy conservation condition in Eq. (1), since here a mean-field dispersion relation for the density excitation is sufficient. Writing $\Phi(\mathbf{r}) \equiv \langle \hat{\psi}(\mathbf{r}) \rangle = \phi_0(\mathbf{r}) + \delta\phi(\mathbf{r})$, with $\phi_0(\mathbf{r})$ being the ground-state wave function and noting that the relevant process involves mainly phonons in the low-momentum regime, we can write $\epsilon_{\mathbf{k}} = c_{\theta_{\mathbf{k}}}k$ for a phonon carrying momentum \mathbf{k} , with $k = |\mathbf{k}|$. Here, $c_{\theta_{\mathbf{k}}}$ is the sound velocity, which for the Hamiltonian (3) is found as $c_{\theta_{\mathbf{k}}} = \sqrt{1/\kappa m^*}$ [54], where $\kappa^{-1} = 2G_1$ is the compressibility [55] and m^* is the effective mass [56] given by

$$\frac{m}{m^*} = 1 - \frac{2\hbar^2 k_0^2 \cos^2 \theta_{\mathbf{k}}}{m(4G_2 + \hbar\Omega)}. \quad (5)$$

Here $\theta_{\mathbf{k}}$ measures the angle between the direction of momentum \mathbf{k} of a quasiparticle and the x axis (along which SOC is applied). A crucial feature of the effective mass (5) is its spatial anisotropy: $m^* = m$ when \mathbf{k} is perpendicular to the SOC direction, while $m^* > m$ otherwise, as experimentally demonstrated [43]. Notice that m^* exhibits dependence on the spin-dependent interaction G_2 , which for $G_2 = 0$ reduces to the result in Ref. [55]. Thus, the energy conservation condition becomes strongly anisotropic, which for phonons takes the form $c_{\theta_{\mathbf{q}}}q = c_{\theta_{\mathbf{p}}}p + c_{\theta_{\mathbf{q}-\mathbf{p}}}\|\mathbf{q}-\mathbf{p}\|$ [57].

The anisotropic energy condition results in an anisotropic distribution of scattering states contributing to Beliaev decay. To visualize this, we numerically solve the condition $\epsilon_{\mathbf{q}} = \epsilon_{\mathbf{p}} + \epsilon_{\mathbf{q}-\mathbf{p}}$. We will hereafter denote $\theta_{\mathbf{q}} = \theta$, i.e., the angle between the initial momentum \mathbf{q} and the x direction. Figure 1(b) presents the results of an energetically allowed scattered momentum \mathbf{p} manifold for various θ on the $p_x - p_z$ plane ($q_y = p_y = 0$ is taken). Interestingly, we see that the counterclockwise rotation of the manifold is accompanied by an increase of the manifold size with θ , indicating anisotropic distribution of contributing states, in contrast to the SOC-free counterpart where the contour size stays invariant [5].

Next, we discuss the scattering matrix in Eq. (1), which instead requires beyond-mean-field treatment. We follow the approach in Ref. [46], which, by decomposing the total field operator $\hat{\psi} = \Phi + \tilde{\psi}$, where $\tilde{\psi}$ annihilates noncondensate atoms and is treated perturbatively, allows for the account of couplings between Bogoliubov quasiparticles

and noncondensate atoms. In this framework (see Supplemental Material [44]), the matrix element $B_{\mathbf{p}\mathbf{p}'}$ in terms of usual Bogoliubov amplitudes $u(v)$ reads $B_{\mathbf{p}\mathbf{p}'} = \tilde{B}_{\mathbf{p}\mathbf{p}'} + \tilde{B}_{\mathbf{p}'\mathbf{p}}$, with

$$\begin{aligned} \tilde{B}_{\mathbf{p}\mathbf{p}'} = & \sqrt{\frac{n_0}{2V}} \sum_{\alpha=1,2} (-1)^{\alpha+1} \{ [g(2u_{\alpha,\mathbf{p}}v_{\alpha,\mathbf{p}'} + u_{\alpha,\mathbf{p}}u_{\alpha,\mathbf{p}'}) \\ & + g_{12}(u_{\bar{\alpha},\mathbf{p}}v_{\bar{\alpha},\mathbf{p}'} - u_{\bar{\alpha},\mathbf{p}}u_{\alpha,\mathbf{p}'} - u_{\alpha,\mathbf{p}}v_{\bar{\alpha},\mathbf{p}'})] u_{\alpha,\mathbf{q}} \\ & + [g(2u_{\alpha,\mathbf{p}}v_{\alpha,\mathbf{p}'} + v_{\alpha,\mathbf{p}}v_{\alpha,\mathbf{p}'}) \\ & + g_{12}(u_{\bar{\alpha},\mathbf{p}}v_{\bar{\alpha},\mathbf{p}'} - v_{\bar{\alpha},\mathbf{p}}v_{\alpha,\mathbf{p}'} - v_{\alpha,\mathbf{p}}u_{\bar{\alpha},\mathbf{p}'})] v_{\alpha,\mathbf{q}} \}. \quad (6) \end{aligned}$$

We will now take an experimental viewpoint by describing Eq. (6) in terms of the dynamic structure factors [4], as inspired by Ref. [6]. In cold atom experiments, the dynamic structure factor can be directly measured by means of Bragg spectroscopy [7,58–60] or *in situ* imaging [61,62], as in recent studies of SOC BECs [43,63,64], which gives experimental access to the Bogoliubov amplitudes $u(v)$ [65,66]. A SOC BEC has two types of dynamic structure factor [42,55], i.e., the density and spin-density dynamic structure factors, describing the system response to the density and spin-density perturbations, respectively. Formally, the density dynamic structure factor is given by $S_d(\mathbf{q}, \omega) = N^{-1} \sum_n |\langle 0 | \rho_{\mathbf{q}} | n \rangle|^2 \delta(\omega - \omega_{n0})$, where $\rho_{\mathbf{q}} = \sum_i e^{i\mathbf{q}\cdot\mathbf{x}_i}$ is the density operator with momentum \mathbf{q} and ω_{n0} is the excitation frequency of the n th state, while the spin-density dynamic structure factor is $S_s(\mathbf{q}, \omega) = N^{-1} \sum_n |\langle 0 | s_{\mathbf{q}} | n \rangle|^2 \delta(\omega - \omega_{n0})$, with $s_{\mathbf{q}} = \sum_i \sigma_{z_i} e^{i\mathbf{q}\cdot\mathbf{x}_i}$ being the standard spin-density operator. The static density and spin-density structure factor are thus $S_{d(s)}(\mathbf{q}) = \int d\omega S_{d(s)}(\mathbf{q}, \omega)$, with $S_d + S_s = 1$.

Without SOC, the density and spin-density excitations of a two-component BEC are decoupled, so that an external density perturbation $\delta\hat{\rho}$ acting on BECs only induces a density response in the form of the density dynamic structure factor. Instead, due to the absence of Galilean invariance in a SOC BEC, a density perturbation along the x direction in the system, which formally corresponds to a gauge transformation $e^{iq_x x}$ [4], will concomitantly induce a velocity-dependent Zeeman-energy term $-q_x \hbar k_0 \sigma_z$, resulting in generations of both density and spin-density responses.

Figures 1(c) and 1(d) compare $S_d(\mathbf{q})$ [Fig. 1(c)] and $S_s(\mathbf{q})$ [Fig. 1(d)] for various SOC strength k_0 , taking $\theta = 0$. Without SOC, it is well known that S_d asymptotically approaches unity at large momenta, while S_s is pinned to zero (see blue solid curves). In contrast, the most prominent feature in the presence of SOC is that S_s becomes finite at all momenta, signaling the coupling of density and spin-density excitations. In particular, at large momenta, both S_d and S_s unanimously approach 1/2 [see insets of Figs. 1(c) and 1(d)]. Such different asymptotic behavior compared to the SOC-free case can be analytically understood as

follows: the static structure factor can be written as $S_d = N^{-1} |\sum_{\alpha=1,2} \sqrt{n_{i0}} (u_{\alpha\mathbf{q}} + v_{\alpha\mathbf{q}})|^2$ and $S_s = N^{-1} |\sum_{\alpha=1,2} \sqrt{n_{\alpha 0}} \text{sgn}(\alpha) (u_{\alpha\mathbf{q}} + v_{\alpha\mathbf{q}})|^2$, with $\text{sgn}(1) = -\text{sgn}(2) = 1$. For $q \rightarrow \infty$, when $k_0 = 0$, we have $u_{1\mathbf{q}} = v_{1\mathbf{q}} = 1/\sqrt{2}$ and $u_{2\mathbf{q}} = v_{2\mathbf{q}} = 0$. On the other hand, when $k_0 \neq 0$, we have $u_{1\mathbf{q}} \rightarrow 1$, $v_{1\mathbf{q}} \rightarrow 0$, and $u_{2\mathbf{q}} = v_{2\mathbf{q}} = 0$. At small momenta, we see that the increase rate S_s enhances with k_0 as expected. For arbitrary momenta, the Bogoliubov amplitudes u and v in Eq. (6) can be related to S_d and S_s as [67]

$$u_{\alpha,\mathbf{q}} = \frac{f + (-1)^{\alpha+1} 2\beta_q \{[\sqrt{S_d} + (-1)^{\alpha+1} \sqrt{S_s}]^2 + 1\}}{4\sqrt{2}[\sqrt{S_d} + (-1)^{\alpha+1} \sqrt{S_s}]\beta_q},$$

$$v_{\alpha,\mathbf{q}} = \frac{-f + (-1)^{\alpha+1} 2\beta_q \{[\sqrt{S_d} + (-1)^{\alpha+1} \sqrt{S_s}]^2 - 1\}}{4\sqrt{2}[\sqrt{S_d} + (-1)^{\alpha+1} \sqrt{S_s}]\beta_q}.$$

Thus, by measuring the dynamic structure factor and hence accessing Bogoliubov amplitudes [65,66], one can access the matrix element in Eq. (6) for the SOC BEC, along the lines of the Beliaev damping experiments in the one-component BEC [6].

Finally, in performing the summation in Eq. (1), we will assume all momenta are along the same direction [5,7], i.e., $\theta_{\mathbf{q}} = \theta_{\mathbf{p}} = \theta_{\mathbf{p}-\mathbf{q}} = \theta$, as collisions at zero temperature dominantly occur in the low-momentum regime, where the energy and momentum conservation conditions require the scattered momentum \mathbf{p} be parallel with the initial momentum \mathbf{q} . This way, straightforward evaluation gives (see Supplemental Material [44])

$$\gamma_B = \gamma_0 \left(1 - \frac{2\hbar^3 \Omega k_0^2 \cos^2 \theta}{m(4G_2 + \hbar\Omega)^2}\right)^2 \sqrt{1 + \chi_M \frac{\hbar^2 k_0^2}{m} \sin^2 \theta}. \quad (7)$$

Here χ_M is the spin polarizability susceptibility [54,55], which takes the form

$$\chi_M = \frac{2}{(\hbar\Omega + 4G_2) - 2\hbar^2 k_0^2/m}. \quad (8)$$

Equation (7) is the key result of this Letter. Apparently, γ_B for $k_0 = 0$ reduces to γ_0 of the SOC-free counterpart [see Eq. (2)]. While maintaining the familiar q^5 dependence [see Fig. 2(a)], γ_B displays the following distinguishing features in contrast to γ_0 :

(i) γ_B is explicitly interaction dependent, which comes in only via $g - g_{12}$ (contained in G_2) characterizing the strength of spin-density interaction [see Eq. (3)]. This presents a clear manifestation of the coupled density and spin-density excitations due to SOC on phonon dissipations. Interestingly, γ_B at $\theta \neq 0$ exhibits a characteristic divergence at the critical point $4G_2 + \hbar\Omega = 2\hbar^2 k_0^2/m$, which is just the aforementioned phase boundary between the zero-momentum and plane wave phases. This divergence

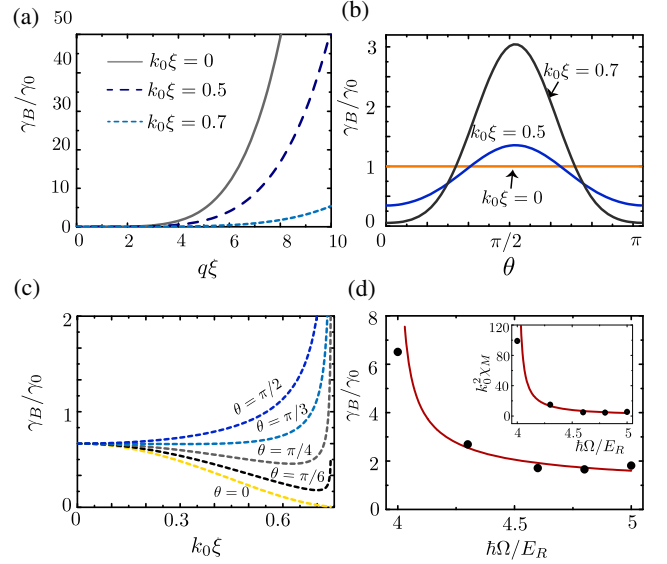


FIG. 2. The Beliaev damping rate γ_B as a function of (a) the modulus of momentum $q = |\mathbf{q}|$, fixing $\theta = 0$; (b) the angle θ , taking $q\xi = 0.8$; (c) the SOC strength k_0 with $G_1/\hbar\Omega = 0.1$; $G_2/\hbar\Omega = 0.025$ (d) the $\hbar\Omega$, taking $\theta = \pi/3$, $G_2 = 0$, and $E_R = \hbar^2 k_0^2/2m$. The solid lines and black dots in (d) correspond to the theoretical predictions and the experimental data in Ref. [26], respectively.

of γ_B comes from the divergence of spin polarizability susceptibility χ_M . As discussed earlier, a density perturbation due to presence of SOC is necessarily accompanied by a perturbation $\sim \sigma_z$. This induces a system response in form of the spin polarizability susceptibility, which has been shown to be able to distinguish the unpolarized zero-momentum phase and the spin-polarized plane wave phase. Note that the measurement of spin polarizability for the considered SOC BEC has been recently reported [26]. By contrast, γ_B at $\theta = 0$ always stays finite. This can be understood by noticing that the effective mass along the SOC direction diverges [see Eq. (5)], giving rise to the so-called phonon softening [43], which at the phase boundary effectively cancels the divergence of χ_M . We note that the determination of condensate density n_0 in Eq. (7) relies on the density interaction constant $g + g_{12}$ [33].

(ii) γ_B is strongly anisotropic depending on the angle between initial momentum \mathbf{q} of quasiparticle and SOC direction, which can be understood in terms of the SOC-induced anisotropic effective mass. In fact, Eq. (7) can be cast into a more transparent form by ignoring G_2 , i.e.,

$$\gamma_B = \left(\frac{3q^5}{640\pi\hbar^3 m^* n_0}\right) \frac{m}{m^*} \sqrt{1 + \chi_M \frac{\hbar^2 k_0^2}{m} \sin^2 \theta}. \quad (9)$$

Thus, for a fixed SOC strength k_0 , the decay of the quasiparticle is most significant when \mathbf{q} is perpendicular to the SOC direction, but is strongly suppressed when the two are parallel [see Fig. 2(b)]. In addition, when increasing

SOC [see Fig. 2(c)], the decay along the SOC direction is increasingly suppressed, while that in the perpendicular direction is enhanced, although for other directions, γ_B is generally nonmonotonic with respect to k_0 .

Experimental realization and discussions.—In experiments on SOC BEC [26], the measurement of spin polarizability susceptibility χ_M in Eq. (8) had been performed by variations of Raman coupling, i.e., $\hbar\Omega$; see black dots in the inset of Fig. 2(d). Equation (7) therefore allows immediate experimental access of the Beliaev decay rate through the measurement of χ_M . In Fig. 2(d), we demonstrate how the Beliaev damping rate varies with the $\hbar\Omega$, where the black dots correspond to the experimental data of χ_M [26]. Further, in view of the fact that the measurement of bare damping rate γ_0 has been achieved [5–7] and that $\gamma_B > \gamma_0$, we anticipate the phenomena discussed in this Letter should be observable within the current experimental capabilities.

We have shown how the effect of SOC can manifest itself in the Beliaev damping of low-energy excitations of a BEC, even when the ground state is in the zero-momentum phase, and the essential features such as anisotropy and the dependence on the spin density should also be seen in the plane wave phase and the stripe phase. In the latter phases, since the ground-state wave functions and the single-particle dispersions already bear clear signatures of the SOC effect (unlike the zero-momentum phase), the explorations of the unique features of quasiparticle decay there remain an open challenge. In addition, our analysis connects the damping rate with the presently detectable dynamical structure factors, and thus opens the possibility for experimental access, e.g., by means of Bragg spectroscopy [43]. While many-body quantum systems with SOC have been intensively studied within the mean-field framework, observing the Beliaev damping in a SOC BEC would present an important step toward revealing the interplay between the non-Abelian gauge fields and the beyond-mean effects. Along this direction, further investigations include, e.g., the lifetime of quasiparticles at finite temperatures in SOC BECs.

We would like to thank W. Vincent Liu, Zengqiang Yu, Biao Wu, Hua Chen, Chao Gao, Xianlong Gao, Ying Hu, and Wei Yi for stimulating discussions. This work is financially supported by the National Natural Science Foundation of China (Grants No. 11274315, 11774316 and 61227902), the key projects of the Natural Science Foundation of China (Grant No. 11835011), the National Key R & D Program of China (Grant No. 2016YFA0301500) and Zhejiang Provincial Natural Science Foundation of China under Grant No. LQ13A040005.

*Corresponding author.
zhxliang@gmail.com

[1] X. Wen, *Quantum Field Theory of Many-Body Systems* (Oxford University Press, Oxford, 2004).

- [2] S. T. Beliaev, Application of the methods of quantum field theory to a system of bosons, *Sov. Phys. JETP* **7**, 289 (1958).
- [3] S. T. Beliaev, Energy-spectrum of a non-ideal Bose gas, *Sov. Phys. JETP* **7**, 299 (1958).
- [4] P. Nozieres and D. Pines, *The Theory of Quantum Liquids* (Addison-Wesley, New York, 1990), Vol. II.
- [5] E. Hodby, O. M. Maragò, G. Hechenblaikner, and C. J. Foot, Experimental Observation of Beliaev Coupling in a Bose-Einstein Condensate, *Phys. Rev. Lett.* **86**, 2196 (2001).
- [6] N. Katz, J. Steinhauer, R. Ozeri, and N. Davidson, Beliaev Damping of Quasiparticles in a Bose-Einstein Condensate, *Phys. Rev. Lett.* **89**, 220401 (2002).
- [7] R. Ozeri, N. Katz, J. Steinhauer, and N. Davidson, Colloquium, *Rev. Mod. Phys.* **77**, 187 (2005).
- [8] Y. Kawaguchi and M. Ueda, Spinor Bose-Einstein condensates, *Phys. Rep.* **520**, 253 (2012).
- [9] W. Zheng and H. Zhai, Quasiparticle Lifetime in a Mixture of Bose and Fermi Superfluids, *Phys. Rev. Lett.* **113**, 265304 (2014).
- [10] H. Shen and W. Zheng, Landau damping in a mixture of Bose and Fermi superfluids, *Phys. Rev. A* **92**, 033620 (2015).
- [11] J. H. Pixley, X. Li, and S. Das Sarma, Damping of Long-Wavelength Collective Modes in Spinor Bose-Fermi Mixtures, *Phys. Rev. Lett.* **114**, 225303 (2015).
- [12] S. K. Yip, Collective modes in a dilute Bose-Fermi mixture, *Phys. Rev. A* **64**, 023609 (2001).
- [13] D. H. Santamore, S. Gaudio, and E. Timmermans, Zero Sound in a Mixture of a Single-Component Fermion Gas and a Bose-Einstein Condensate, *Phys. Rev. Lett.* **93**, 250402 (2004).
- [14] D. H. Santamore and E. Timmermans, Collective excitations of low-density fermion-boson quantum-liquid mixtures, *Phys. Rev. A* **72**, 053601 (2005).
- [15] X.-J. Liu and H. Hu, Finite-temperature excitations of a trapped Bose-Fermi mixture, *Phys. Rev. A* **68**, 033613 (2003).
- [16] S. S. Natu and S. Das Sarma, Absence of damping of low-energy excitations in a quasi-two-dimensional dipolar Bose gas, *Phys. Rev. A* **88**, 031604 (2013).
- [17] S. S. Natu and R. M. Wilson, Landau damping in a collisionless dipolar Bose gas, *Phys. Rev. A* **88**, 063638 (2013).
- [18] R. M. Wilson and S. Natu, Beliaev damping in quasi-two-dimensional dipolar condensates, *Phys. Rev. A* **93**, 053606 (2016).
- [19] M. Van Regemortel, W. Casteels, I. Carusotto, and M. Wouters, Spontaneous Beliaev-Landau scattering out of equilibrium, *Phys. Rev. A* **96**, 053854 (2017).
- [20] M.-C. Chung and A. B. Bhattacharjee, Dynamical Structure Factor and Spin-Density Separation for a Weakly Interacting Two-Component Bose Gas, *Phys. Rev. Lett.* **101**, 070402 (2008).
- [21] A. B. Bhattacharjee, Damping in two-component Bose gas, *Mod. Phys. Lett. B* **28**, 1450029 (2014).
- [22] Y. J. Lin, R. L. Compton, K. Jimenez-Garcia, J. V. Porto, and I. B. Spielman, Synthetic magnetic fields for ultracold neutral atoms, *Nature (London)* **462**, 628 (2009).
- [23] Y. J. Lin, K. Jimenez-Garcia, and I. B. Spielman, Spin-orbit-coupled Bose-Einstein condensates, *Nature (London)* **471**, 83 (2011).

- [24] P. Wang, Z.-Q. Yu, Z. Fu, J. Miao, L. Huang, S. Chai, H. Zhai, and J. Zhang, Spin-Orbit Coupled Degenerate Fermi Gases, *Phys. Rev. Lett.* **109**, 095301 (2012).
- [25] L. W. Cheuk, A. T. Sommer, Z. Hadzibabic, T. Yefsah, W. S. Bakr, and M. W. Zwierlein, Spin-Injection Spectroscopy of a Spin-Orbit Coupled Fermi Gas, *Phys. Rev. Lett.* **109**, 095302 (2012).
- [26] J.-Y. Zhang, S.-C. Ji, Z. Chen, L. Zhang, Z.-D. Du, B. Yan, G.-S. Pan, B. Zhao, Y.-J. Deng, H. Zhai, S. Chen, and J.-W. Pan, Collective Dipole Oscillations of a Spin-Orbit Coupled Bose-Einstein Condensate, *Phys. Rev. Lett.* **109**, 115301 (2012).
- [27] S.-C. Ji, J.-Y. Zhang, L. Zhang, Z.-D. Du, W. Zheng, Y.-J. Deng, H. Zhai, S. Chen, and J.-W. Pan, Experimental determination of the finite-temperature phase diagram of a spin-orbit coupled Bose gas, *Nat. Phys.* **10**, 314 (2014).
- [28] J. Li, W. Huang, B. Shteynas, S. Burchesky, F. Ç. Top, E. Su, J. Lee, A. O. Jamison, and W. Ketterle, Spin-Orbit Coupling and Spin Textures in Optical Superlattices, *Phys. Rev. Lett.* **117**, 185301 (2016).
- [29] J.-R. Li, J. Lee, W. Huang, S. Burchesky, B. Shteynas, F. Çagri Top, A. O. Jamison, and W. Ketterle, A stripe phase with supersolid properties in spin-orbit-coupled Bose-Einstein condensates, *Nature (London)* **543**, 91 (2017).
- [30] J. Dalibard, F. Gerbier, G. Juzeliūnas, and P. Öhberg, Colloquium: Artificial gauge potentials for neutral atoms, *Rev. Mod. Phys.* **83**, 1523 (2011).
- [31] V. Galitski and I. B. Spielman, Spin-orbit coupling in quantum gases, *Nature (London)* **494**, 49 (2013).
- [32] H. Zhai, Spin-orbit coupled quantum gases, *Int. J. Mod. Phys. B* **26**, 1230001 (2012).
- [33] W. Zheng, Z.-Q. Yu, X. Cui, and H. Zhai, Properties of Bose gases with the raman-induced spin-orbit coupling, *J. Phys. B* **46**, 134007 (2013).
- [34] N. Goldman, G. Juzeliūnas, P. Öhberg, and I. B. Spielman, Light-induced gauge fields for ultracold atoms, *Rep. Prog. Phys.* **77**, 126401 (2014).
- [35] H. Zhai, Degenerate quantum gases with spin-orbit coupling: A review, *Rep. Prog. Phys.* **78**, 026001 (2015).
- [36] Y. Zhang, M. E. Mossman, T. Busch, P. Engels, and C. Zhang, Properties of spin-orbit-coupled Bose-Einstein condensates, *Front. Phys.* **11**, 118103 (2016).
- [37] L. Dong, L. Jiang, H. Hu, and H. Pu, Finite-momentum dimer bound state in a spin-orbit-coupled Fermi gas, *Phys. Rev. A* **87**, 043616 (2013).
- [38] Q. Zhu, C. Zhang, and B. Wu, Exotic superfluidity in spin-orbit coupled Bose-Einstein condensates, *Europhys. Lett.* **100**, 50003 (2012).
- [39] Q. Zhu and B. Wu, Superfluidity of Bose-Einstein condensates in ultracold atomic gases, *Chin. Phys. B* **24**, 050507 (2015).
- [40] C. Wang, C. Gao, C.-M. Jian, and H. Zhai, Spin-Orbit Coupled Spinor Bose-Einstein Condensates, *Phys. Rev. Lett.* **105**, 160403 (2010).
- [41] Y. Li, L. P. Pitaevskii, and S. Stringari, Quantum Tricriticality and Phase Transitions in Spin-Orbit Coupled Bose-Einstein Condensates, *Phys. Rev. Lett.* **108**, 225301 (2012).
- [42] Y. Li, G. I. Martone, L. P. Pitaevskii, and S. Stringari, Superstripes and the Excitation Spectrum of a Spin-Orbit-Coupled Bose-Einstein Condensate, *Phys. Rev. Lett.* **110**, 235302 (2013).
- [43] S.-C. Ji, L. Zhang, X.-T. Xu, Z. Wu, Y. Deng, S. Chen, and J.-W. Pan, Softening of Roton and Phonon Modes in a Bose-Einstein Condensate with Spin-Orbit Coupling, *Phys. Rev. Lett.* **114**, 105301 (2015).
- [44] See Supplemental Material at <http://link.aps.org/supplemental/10.1103/PhysRevLett.121.180401> for the detailed derivations of Eqs. (1), (6) and (7) in the maintext, which includes Refs. [6,41,46,47].
- [45] W. V. Liu, Theoretical Study of the Damping of Collective Excitations in a Bose-Einstein Condensate, *Phys. Rev. Lett.* **79**, 4056 (1997).
- [46] S. Giorgini, Damping in dilute Bose gases: A mean-field approach, *Phys. Rev. A* **57**, 2949 (1998).
- [47] S. Giorgini, Collisionless dynamics of dilute Bose gases: Role of quantum and thermal fluctuations, *Phys. Rev. A* **61**, 063615 (2000).
- [48] For uniform one-component BEC, the n_0 can be written as $n_0 = n - n_{ex}$ with n and $n_{ex}/n = (8/3\sqrt{\pi})(na_s^3)^{1/2}$ being the total density and quantum depletion, respectively. The Beliaev damping rate in Eq. (2) is implicitly dependent on the interaction constant $g = 4\pi\hbar^2 a_s/m$ through $n_0 = n - n_{ex}$.
- [49] N. T. Phuc, Y. Kawaguchi, and M. Ueda, Beliaev theory of spinor Bose-Einstein condensates, *Ann. Phys. (Amsterdam)* **328**, 158 (2013).
- [50] G. E. Marti, A. MacRae, R. Olf, S. Lourette, F. Fang, and D. M. Stamper-Kurn, Coherent Magnon Optics in a Ferromagnetic Spinor Bose-Einstein Condensate, *Phys. Rev. Lett.* **113**, 155302 (2014).
- [51] T.-L. Ho and S. Zhang, Bose-Einstein Condensates with Spin-Orbit Interaction, *Phys. Rev. Lett.* **107**, 150403 (2011).
- [52] W. Li, L. Chen, Z. Chen, Y. Hu, Z. Zhang, and Z. Liang, Probing the flat band of optically trapped spin-orbital-coupled Bose gases using Bragg spectroscopy, *Phys. Rev. A* **91**, 023629 (2015).
- [53] Z. Chen and Z. Liang, Ground-state phase diagram of a spin-orbit-coupled bosonic superfluid in an optical lattice, *Phys. Rev. A* **93**, 013601 (2016).
- [54] Y. Li, G. I. Martone, and S. Stringari, Sum rules, dipole oscillation and spin polarizability of a spin-orbit coupled quantum gas, *Europhys. Lett.* **99**, 56008 (2012).
- [55] G. I. Martone, Y. Li, L. P. Pitaevskii, and S. Stringari, Anisotropic dynamics of a spin-orbit-coupled Bose-Einstein condensate, *Phys. Rev. A* **86**, 063621 (2012).
- [56] Z. X. Liang, X. Dong, Z. D. Zhang, and B. Wu, Sound speed of a Bose-Einstein condensate in an optical lattice, *Phys. Rev. A* **78**, 023622 (2008).
- [57] For the analysis of the scattering matrix, the phonon dispersion needs to be modified by including a nonlinear term [46], i.e., $\epsilon_{\mathbf{q}} = c_{\theta_{\mathbf{q}}} q + d_{\theta_{\mathbf{q}}} q^3$.
- [58] D. M. Stamper-Kurn, A. P. Chikkatur, A. Görlitz, S. Inouye, S. Gupta, D. E. Pritchard, and W. Ketterle, Excitation of Phonons in a Bose-Einstein Condensate by Light Scattering, *Phys. Rev. Lett.* **83**, 2876 (1999).
- [59] J. Steinhauer, R. Ozeri, N. Katz, and N. Davidson, Excitation Spectrum of a Bose-Einstein Condensate, *Phys. Rev. Lett.* **88**, 120407 (2002).

- [60] X. Du, S. Wan, E. Yesilada, C. Ryu, D.J. Heinzen, Z. Liang, and B. Wu, Bragg spectroscopy of a superfluid Bose-Hubbard gas, *New J. Phys.* **12**, 083025 (2010).
- [61] C.-L. Hung, X. Zhang, L.-C. Ha, S.-K. Tung, N. Gemelke, and C. Chin, Extracting density-density correlations from *in situ* images of atomic quantum gases, *New J. Phys.* **13**, 075019 (2011).
- [62] C.-L. Hung, V. Gurarie, and C. Chin, From cosmology to cold atoms: Observation of Sakharov oscillations in a quenched atomic superfluid, *Science* **341**, 1213 (2013).
- [63] M. A. Khamehchi, Y. Zhang, C. Hamner, T. Busch, and P. Engels, Measurement of collective excitations in a spin-orbit-coupled Bose-Einstein condensate, *Phys. Rev. A* **90**, 063624 (2014).
- [64] L.-C. Ha, L. W. Clark, C. V. Parker, B. M. Anderson, and C. Chin, Roton-Maxon Excitation Spectrum of Bose Condensates in a Shaken Optical Lattice, *Phys. Rev. Lett.* **114**, 055301 (2015).
- [65] A. Brunello, F. Dalfovo, L. Pitaevskii, and S. Stringari, How to Measure the Bogoliubov Quasiparticle Amplitudes in a Trapped Condensate, *Phys. Rev. Lett.* **85**, 4422 (2000).
- [66] J. M. Vogels, K. Xu, C. Raman, J. R. Abo-Shaeer, and W. Ketterle, Experimental Observation of the Bogoliubov Transformation for a Bose-Einstein Condensed Gas, *Phys. Rev. Lett.* **88**, 060402 (2002).
- [67] $f = L - \sqrt{L^2 + 4\beta_q^2 - 4\beta_q \sqrt{S_d S_s} [(\hbar^2 q^2 / 2m) + 2gn_0 + \hbar\Omega]}$
 and $L = S_d(\hbar^2 q^2 / 2m + 4G_1) + S_s(\hbar^2 q^2 / 2m + 4G_2 + \hbar\Omega)$
 and $\beta_q = \hbar k_0 q_x / m$.